Published in final edited form as:
J Control Release. 2007 April 2; 118(2): 235–244.

Factors modulating the delivery and effect of enzymatic cargo conjugated with antibodies targeted to the pulmonary endothelium

Vladimir V. Shuvaev[a,1], **Melpo Christofidou-Solomidou**[b,1], **Arnaud Scherpereel**[a,c], **Eric Simone**[f], **Evguenia Arguiri**[b], **Samira Tliba**[a], **Jeremy Pick**[a], **Stephen Kennel**[d], **Steven M. Albelda**[b], and **Vladimir R. Muzykantov**[a,e,#]

a *Institute for Environmental Medicine, University of Pennsylvania School of Medicine, Philadelphia, PA, 19104, USA*

b *Pulmonary Critical Care Division, Department of Medicine, University of Pennsylvania School of Medicine, Philadelphia, PA, 19104, USA*

c *INSERM U774, Institute Pasteur de Lille, France*

d *University of Tennessee Graduate School of Medicine, Knoxville, TN 37920, USA*

e *Department of Pharmacology and Program in Targeted Therapeutics, Institute of Translational Medicine and Therapeutics, University of Pennsylvania School of Medicine, Philadelphia, PA, 19104, USA*

f *Department of Bioengineering, School of Engineering, University of Pennsylvania*

Abstract

Vascular drug targeting may improve therapies, yet a thorough understanding of the factors that regulate effects of drugs directed to the endothelium is needed to translate this approach into the clinical domain. To define factors modulating the efficacy and effects of endothelial targeting, we used a model enzyme (glucose oxidase, GOX) coupled with monoclonal antibodies (anti-TM_{34} or anti-TM_{201}) to distinct epitopes of thrombomodulin, a surface determinant enriched in the pulmonary endothelium. GOX delivery results in conversion of glucose and oxygen into H_2O_2 leading to lung damage, a clear physiologic endpoint. Results of in vivo studies in mice showed that the efficiency of cargo delivery and its effect are influenced by a number of factors including: 1) The level of pulmonary uptake of the targeting antibody (anti-TM_{201} was more efficient than anti-TM_{34}); 2) The amount of an active drug delivered to the target; 3) The amount of target antigen on the endothelium (animals with suppressed TM levels showed less targeting); and, 4) The substrate availability for the enzyme cargo in the target tissue (hyperoxia augmented GOX-induced injury). Therefore, both activity of the conjugates and biological factors control targeting and effects of enzymatic cargo. Understanding the nature of such “modulating biological factors” will hopefully allow optimization and ultimately applications of drug targeting for “individualized” pharmacotherapy.

[#]Corresponding author. Institute for Environmental Medicine, University of Pennsylvania Medical Center, 1 John Morgan Building, 36th Street and Hamilton Walk, Philadelphia, PA 19104-6068. Phone: 215-898-9823, FAX: 215-898-0868, e-mail address: muzykant@mail.med.upenn.edu.
[1]These authors contributed equally to the study.

Keywords

Vascular immunotargeting; endothelium; thrombomodulin; drug delivery; lungs; oxidative stress

1. Introduction

Targeted drug delivery to the endothelium may help to improve treatment of diseases affecting the vasculature [1–7]. Targeted drug delivery systems (DDSs) designed to achieve this goal consist of affinity vectors (e.g., antibodies directed to endothelial surface determinants) coupled either directly to pharmacological cargoes (e.g., therapeutic enzymes) or to drug-loaded vehicles or carriers (e.g., liposomes or polymer nanocarriers) [8–14]. Endothelial targeting of DDSs carrying reporter probes, enzymes, other drugs, genes and/or drug nanocarriers has been achieved in a number of animal species and even in a few "proof of principal" human studies (reviewed in [1,8]). However, before this approach can move into the clinical domain, a more thorough understanding of the factors that regulate the effects of drugs targeted to endothelium is needed.

Endothelial targeting and effects of DDSs carrying cargo enzymes are regulated by a complex network of factors, some of which are schematized in Figure 1. Features of the target endothelial bed ("Target determinant properties" such as tissue specificity, surface density and accessibility of the target epitope) and elements of the specific drug delivery system design (such as the affinity and valence of the antibody and the size, charge and stealth features of the conjugate) combine to control delivery parameters such as the pharmacokinetics, clearance and targeting of the conjugate, and the ultimate subcellular localization of the cargo within the endothelial cell [8]. Even after successful delivery, the amplitude and duration of the outcome effects of targeting will be affected by the activity and stability of DDS-loaded cargo enzyme and biological factors within the target that regulate rate of supply of enzymatic substrate and tissue sensitivity to products of enzymatic activity. A better understanding of this complex matrix will be needed to optimize targeted drug delivery to the endothelium.

This study will present experiments that begin to define some of the biological factors and elements of DDS design that regulate the targeting and effects of an enzymatic cargo in the pulmonary vasculature, an important target for pharmacological interventions [1,3,15,16]. To achieve this goal, we utilized an enzyme (glucose oxidase, GOX, that generates H_2O_2 from O_2 and glucose) as a model cargo coupled with well-characterized antibodies to an endothelial determinant enriched in the lungs, thrombomodulin (TM) [17]. We have previously showed that anti-TM/GOX conjugates accumulate in the lungs after IV injection and within a few hours cause local effects manifested by pulmonary edema due to vascular oxidative injury induced by H_2O_2 [18,19].

In this study, we used two different monoclonal antibodies to TM: mAb anti-TM34-211 (anti-TM_{34}) and anti-TM201-411 (anti-TM_{201}), which are directed to distinct TM epitopes and have different affinities for TM [20]. We conjugated GOX to anti-TM mAbs via either a streptavidin cross-linker to produce anti-TM/GOX conjugates (~300 nm diameter), or by coating GOX and anti-TM to the surface of polystyrene beads to produce anti-TM/bead/GOX formulations (~200 nm diameter). We then utilized these conjugates to evaluate the effects of: i) the binding features of antibodies and design of DDS (Fig. 1, Blocks I and II); ii) the importance of the level of expression of the target determinant (Fig.1, Block 1, B); and iii) the tissue supply of GOX substrate, O_2 (Fig.1, Block V, A).

2. Materials and Methods

2.1. Reagents

The following materials were used in the study: dimethyl formamide (DMF), rat IgG, glucose oxidase (GOX) from *Aspergillus niger*, protease inhibitor cocktail from Sigma (St. Louis, MO); streptavidin (SA) from *Streptomyces avidinii* from Calbiochem (San Diego, CA); 2-(4'-hydroxyazobenzene) benzoic acid (HABA), succinimidyl-6-(biotinamido) hexanoate (NHS-LC-Biotin), avidin, and iodination reagent IODO-beads form Pierce (Rockford, IL); polystyrene-latex beads 100 nm microspheres from Polysciences (Warrington, PA). Monoclonal antibodies mAb anti-TM34-211 (anti-TM_{34}) and anti-TM201-411 (anti-TM_{201}) are rat antibodies against murine TM, described previously [20–22]. A monoclonal antibody raised in rats against human creatine kinase was used as control IgG (ATCC hybridoma, CKMM 14.15, Manassas, VA).

2.2. Conjugation of glucose oxidase to anti-TM and polymer beads

Immunoglobulins and GOX were modified by a biotinylating reagent, NHS-LC-Biotin, to produce biotinylated derivatives as described previously [23]. Protein concentration was determined by BioRad protein assay (Bio-Rad, Hercules, CA). The level of biotinylation was measured by HABA assay (Pierce, Rockford, IL) in accordance with manufacturer's recommendations. To trace targeting, GOX was labeled with ^{125}Iodine using Iodogen-coated tubes. Protein iodination was performed using the iodination reagent IODO-beads (Pierce, Rockford, IL) in accordance with manufacturer's recommendations. Streptavidin cross-linker was used to produce b-anti-TM/SA/b-GOX or b-IgG/SA/b-GOX, as described in details in previous publications [19,22,24,25]. These conjugates are indicated as anti-TM_{34}/GOX, anti-TM_{201}/GOX or IgG/GOX in the text. In an alternative method, GOX and targeting anti-TM were co-immobilized on the surface of 100 nm diameter polystyrene beads, to produce anti-TM/bead/GOX with final size ~200 nm in diameter, as described [26].

Solid poly(lactic-*co*-glycolic acid) PLGA nanoparticles were prepared by a modified single emulsion technique, as described before [27]. Similar to solvent extraction of microsphere particle preparations reviewed by Freitas et al. [28] and other nanoparticle formulations [29] this nanoprecipitation method involves dissolving PLGA in a water miscible solvent, such as acetone, and addition to a stabilizing surfactant solution. Briefly, a 1 ml solution of 25 mg/ml PLGA in acetone was added dropwise to 6ml of F68 pluronic surfactant under vortexing. Residual acetone was dialyzed against water overnight at 4°C. Nanoparticles were collected by centrifugation at 25,000 g for 30min. This washing step was repeated twice in PBS to remove residual surfactant, and the final particle prep was resuspended and sonicated to break up aggregates. GOX was immobilized on PLGA nanoparticles by the same method used for polystyrene beads.

Enzymatic activity of GOX was measured using an Amplex Red Glucose/Glucose Oxidase Assay Kit (Molecular probe, Eugene, OR).

2.3. Evaluation of anti-TM/GOX conjugate size

In order to minimize confounding effects of size of the conjugates, experiments described in this paper have been performed with GOX conjugates having a mean diameter of 300±20 nm. The size of the conjugates was determined by Dynamic Light Scattering (DLS) using a 90Plus Particle Sizer (Brookhaven Instruments Corp., NY), as described elsewhere [30]. The average particle size was calculated by means of the Stokes-Einstein equation from the diffusion coefficient obtained from a second order cumulative fit to the data. By varying the extent of GOX and anti-TM biotinylation and fine-tuning molar ratios between biotinylated proteins (GOX and antibody) and streptavidin, we produced a series of the conjugates ranging from 50

up to 10,000 nm diameters. GOX and anti-TM were kept at 1:1 molar ratio. Our previous data showed that 300 nm conjugates are optimal for the specific antigen-mediated targeting of the conjugates to pulmonary endothelium, but precludes a non-specific mechanical uptake in the capillaries [30].

2.4. Evaluation of the pulmonary targeting of the conjugates in intact mice

All animal procedures were approved by the Institutional Animal Care and Use Committee (IACUC) of the University of Pennsylvania. Normal C57BL/6 mice (Charles River, NJ) were injected with ~1 μg (~100,000 cpm) of anti-TM/^{125}I-GOX or IgG/^{125}I-GOX in 100 μl saline via tail vein. One hour later, animals were sacrificed; the internal organs were dissected, washed with saline, blotted dry and weighed. Tissue radioactivity in blood and organs was determined in a γ-counter (Wallac-LKB). The results of [^{125}I] measurements in the organs were used to calculate the % of injected dose per gram of tissue (%ID/g).

2.5. Injection of anti-TM/GOX conjugates and characterization of the lung injury

To test effects caused by anti-TM/GOX in mice, we injected 5–50 μg of the immune or non-immune conjugates in anesthetized C57BL/6 mice (Charles River, NJ) intravenously (IV) via tail vein in injection volumes not exceeding 150 μl. Unless specified otherwise, the dose of injected GOX was expressed as μg per gram of mouse body weight. Animals were sacrificed at time-points ranging from 1–24 hours post injection. The lungs were harvested and allocated for histopathology and immunostaining, measurements of biochemical parameters in lung homogenates, wet-to-dry weight ratio and bronchoalveolar lavage (BAL) to test BAL fluid protein concentration. For histopathological studies, the lungs were instilled prior to removal from the animal with 0.75 ml of buffered formalin through a 20-gauge angiocatheter placed in the trachea, immersed in buffered formalin overnight, and then processed for conventional paraffin histology. Sections were stained with hematoxylin and eosin, and examined by light microscopy.

2.6. Evaluation of the protein level in bronchoalveolar lavage fluid (BAL fluid)

BAL was performed by exposing and cannulating the trachea with a 20-gauge angiocatheter (Becton Dickinson; Sandy, UT) and then lavaging three times with 0.5 ml phosphate-buffered saline (PBS) containing a protease inhibitor cocktail (Sigma) at 10 μl per ml. Recovery of infused fluid was >90%. The lavage fluid was spun at 2000 rpm for 3–4 minutes; the supernatant was collected, aliquoted, and frozen at −70°C. Protein concentrations were later measured in the thawed supernatant of the BAL fluid using a standard BCA assay (Pierce Chemicals; Rockford, IL).

2.7. Western blot analysis of thrombomodulin and GOX in lung tissue

Frozen lungs harvested from control mice or animals injected with conjugates (4 h post injection, lungs perfused with buffer prior to harvesting) were homogenized for 1 min with an electric TissueMiser System (Fisher Sci.) in the presence of 400 μl of lysis buffer (0.5% SDS, 0.5% NP40, supplemented with protease inhibitor cocktail) and centrifuged at 4000 rpm (Eppendorf centrifuge) for 10 min at 4ºC. Protein concentrations in the supernatants were measured by BCA assay (Pierce Chemicals; Rockford, IL). Supernatants of lung homogenate were mixed with sample buffer for SDS-PAGE. Samples (10 μg of protein/well) were subjected to 10% SDS-PAGE according to [31]. Gels were transferred to polyvinylidene fluoride (PVDF) membrane (Millipore) using a semi-dry transfer unit (Amersham Pharmacia Biotech). After protein transfer, the PVDF membrane was blocked with 10% nonfat dry milk in Tris-buffered saline, (100 mM Tris (pH 7.5), 150 mM NaCl, 0.1 % Tween 20; TBST) for 1 h and the membrane was treated with primary antibody for overnight (4°C) and corresponding horseradish peroxidase-labeled secondary antibody for 1 h. The blot was washed three times

with TBST and bound horseradish peroxidase was detected using ECL Plus reagents (Amersham Pharmacia Biotech). Thrombomodulin was detected using goat polyclonal anti-TM antibody (M-17, Santa Cruz, CA) followed by reaction with horseradish peroxidase-conjugated donkey anti-goat antibody (Santa Cruz, CA). GOX was detected through its biotin moiety by horseradish peroxidase-conjugated streptavidin (Calbiochem) and actin was estimated using horseradish peroxidase-conjugated anti-actin antibody (I-19, Santa Cruz, CA).

2.8. Hyperoxia exposures

Mice were kept for the duration of the study in cages containing food and water *ad libidum* placed inside a hyperoxic chamber with a continuous flow of O_2 at 10 L/min, yielding O_2 concentrations of 80%–100% as determined by an oxygen analyzer (model 600-ESD; Newark, DE) and described in [32,33].

2.9. Statistical analysis

Statistical differences among groups was determined using one-way analysis of variance (ANOVA). When statistically significant differences were found ($p<0.05$) individual comparisons were made using the Bonferoni/Dunn test (Statview 4.0).

3. Results

3.1. Binding features of the antibodies control amplitude of pulmonary targeting of anti-TM/GOX

Our first goal was to quantify the amplitude of pulmonary targeting achieved 60 min after IV injection of each ^{125}I-labeled anti-TM or each conjugate carrying tracer amounts (~1 μg/mouse) of ^{125}I-GOX. The control IgG, IgG/GOX and IgG/bead/GOX formulations that were used to account for non-specific uptake in the pulmonary vasculature showed no appreciable pulmonary uptake, i.e., lung-to-blood ratio <1 (Fig. 2). In contrast, both anti-TM antibodies showed strong pulmonary targeting with lung-to-blood ratios approaching ~75 for the best formulations (Fig. 2A). Despite effective targeting of either of the antibodies alone, targeting of the conjugates with the TM_{34} antibody were far inferior to the targeting of conjugates made with the TM_{201} antibody. Thus, anti-TM_{201}/125I-GOX and anti-TM_{201}/bead/125I-GOX showed pulmonary uptake that were an order of magnitude higher than the anti-TM_{34}/125I-GOX and anti-TM_{34}/bead/GOX (Fig. 2B and 2C) and achieved 349±27 %ID/g for the best formulation, namely, anti-TM_{201}/bead/125I-GOX. These experiments show that features of the targeting antibody, i.e., affinity and the epitope location, are critical to the efficiency of delivery.

3.2. Targeting effectiveness and enzyme activity control anti-TM/GOX effect

To determine if this difference in the targeting of enzymes by the different antibodies predicted functional efficacy, we analyzed BAL protein levels (as a reflection of pulmonary edema) (Fig. 3A) and assessed lung histopathology using H&E staining of tissue sections (Fig. 3B).

Consistent with more effective targeting, anti-TM_{201}/GOX caused markedly more severe lung injury *vs* anti-TM_{34}/GOX at doses ranging from 0.75 μg/g to 1.5 μg/g, manifested by edema (Fig. 3A), leukocyte infiltrate and alveolar damage (Fig. 3B). Of note, at an intermediate dose, anti-TM_{201}/GOX caused ~5-fold higher elevation of BAL protein level *vs* anti-TM_{34}/GOX (Fig. 3A), which correlates well with the targeting difference of these conjugates (Fig. 2B). The IgG/GOX conjugate that showed no pulmonary targeting did not induce noticeable injury, even at a dose of ~2 μg/g (Fig. 3A, checkered bar on the right). This control confirms that the effect of anti-TM/GOX was due to specific endothelial targeting.

On the other hand, local effect of the targeted enzyme depends on its functional activity. Analysis of the enzymatic activity of GOX formulations showed that biotinylation caused a modest (<20%) reduction in GOX activity due to modification of lysine residues (Fig. 3C). Subsequent conjugation via streptavidin with either anti-TM_{201} or anti-TM_{34} led to additional loss of a similar fraction of GOX activity (20-25% for both conjugates), perhaps due to blocking of GOX by other components of the conjugates. Therefore, both anti-TM/GOX conjugates retained ~60% of GOX activity and comparison of their effect in vivo reflected rather differences in targeting and not in the injected activity of GOX.

In contrast, absorption to polystyrene beads caused a 96% GOX inactivation (Fig. 3C). The loss of enzyme activity explains why anti-TM_{201}/bead/GOX, which displayed the superior targeting features (Fig.2C), caused only marginal lung injury even at the dose of 2 μg/g (Fig. 3A: the far right open bar shows "effect" of anti-TM_{201}/bead/GOX). This unexpected outcome precluded use of this formulation for further functional studies.

Interestingly, coupling of GOX to nanoparticles of similar size based on PLGA, a biocompatible copolymer used for drug delivery purposes [34–36], did not lead to such an overt inactivation (Fig. 3C). It is likely that coupling to a less hydrophobic surface does not inflict as strong denaturing effect on the enzyme. Nevertheless, radioactivity tracing showed that the total amount of GOX that can be loaded on PLGA nanocarriers was 5–7 times lower vs polystyrene counterpart (Fig.3C, inset). Therefore, in terms of total amount of loaded enzymatic activity, PLGA nanocarriers were also suboptimal for delivery of effective doses of GOX. Thus, in the subsequent studies we focused on streptavidin anti-TM/GOX conjugates.

3.3. Level of oxygen supply modulates the effects of anti-TM/GOX

To test the role of the substrate supply in the effect of targeted GOX, we exposed mice to various levels of O_2, the substrate necessary for the enzymatic production of H_2O_2 by GOX. Five minutes after anti-TM/GOX injection, mice were placed in a chamber with regulated inflow of O_2. Importantly, short-term (<20 hours) exposure to elevated level of oxygen (hyperoxia, i.e., O_2 level >80%) does not produce detectable pathological changes in animals, whereas prolonged (i.e., several days) hyperoxia causes oxidative stress and lung damage in animals [32] and human patients [37].

However, a short-term hyperoxia, innocuous by itself, markedly augmented the injurious effect of anti-TM/GOX (Fig. 4). For example, at 80% O_2, lethal lung injury developed within 4 hours after injection of doses of anti-TM_{34}/GOX, a dose that inflicted marginal injury at room air (Fig. 4A). In contrast, hypoxia (10% O_2) significantly reduced the BAL protein level in anti-TM/GOX-treated animals to levels similar to basal amounts seen in naïve control mice (Fig. 4B). This is likely due to the fact that insufficient substrate supply diminishes H_2O_2 production by GOX. Aggravation of anti-TM/GOX injury by hyperoxia was manifested by elevated level of: i) BAL protein (Fig. 4A-D); ii) tissue injury revealed by histopathology evaluation and immunostaining for nitrotyrosine, a marker of oxidative nitrosylation (Fig. 4A, inset); and, iii) accumulation of the products of lipid peroxidation in the lung tissue (Fig. 4B, inset).

To test the effect of duration of hyperoxia exposure, we used moderate doses of anti-TM_{34}/GOX, in order to avoid the acute mortality observed at higher anti-TM/GOX doses in hyperoxia (Fig. 4C). This kinetic study revealed that: i) the maximal extent of lung edema was fully developed by 4 hours at both hyperoxic and room air conditions; and, ii) a more prolonged (24–72 h) hyperoxia exposure did not inflict more profound injury (Fig. 4C).

The effect of hyperoxia was observed with both anti-TM_{34}/GOX and anti-TM_{201}/GOX conjugates. However, consistent with targeting differences (Fig. 2B), anti-TM_{201}/GOX was more potent *vs* anti-TM_{34}/GOX in hyperoxia (Fig. 4D). Interestingly, at high doses, control

IgG/GOX induced some detectable injury in hyperoxia, although much smaller than that produced by anti-TM/GOX. This, targeting-independent, effect was likely due to O_2-mediated stimulation of H_2O_2 production by GOX circulating in the bloodstream.

3.4. Thrombomodulin level in lungs controls the targeting and effect of anti-TM/GOX

After performing ~50 independent experiments, we noticed in several series that some mice were more resistant to anti-TM/GOX injury *vs* the majority of animals within the group. We hypothesized that these fluctuations might reflect, among other factors, individual variability in targeting of the conjugates and/or sensitivity to oxidative stress.

Of note in this context, the endothelial level of TM expression is somewhat labile and is sensitive to diverse factors including cytokines, thrombosis, infections, inflammation and oxidative stress, which all suppress TM expression and stimulate its disappearance from endothelial cells [38]. Figure 5 illustrates this point, showing that pulmonary oxidative stress induced by prolonged hyperoxia reduces the TM level determined by Western-blotting in the lung homogenate (Fig. 5A) and pulmonary uptake of ^{125}I-labeled anti-TM (Fig. 5B). After 48 h hyperoxia, ^{125}I-anti-TM lung-to-blood ratio was reduced ~5-fold vs control (Fig. 5C), consistent with ~5-fold reduction of TM content in the lungs (Fig. 5A). Reduction of pulmonary TM level and suppression of targeting were clear at 48 h hyperoxia, prior to animal morbidity and overt pathological changes in the lung tissue that usually manifest by 72 h of hyperoxia [32]. Based on this data, we posited that some animals utilized in our anti-TM/GOX studies may have low TM levels in the lungs, due to undetected and uncontrolled variations in their health.

We therefore used Western blotting (Fig. 6A) to correlate levels of TM and targeted GOX in the tissue homogenates of lungs obtained from mice that displayed a wide range of variability of injury induced by anti-TM_{34}/GOX in several series and found that: i) TM levels in the lungs of “naïve” mice do vary substantially (Fig. 6A); ii) mice with low endogenous level of TM in the lungs showed proportionally lower targeting of anti-TM/GOX (Fig. 6A,B); iii) this, in turn resulted in a lower extent of lung injury induced by injected anti-TM/GOX (Fig. 6C). Therefore, these interrelationships between TM expression, anti-TM/GOX targeting and effects of anti-TM/GOX help to explain the individual variability in lung injury.

4. Discussion

As targeted drug delivery using antibody conjugates moves beyond the “proof of principle” stage, it is becoming increasingly important to more completely understand the factors that can influence the ultimate therapeutic outcome of this approach. However, as shown in Figure 1, a systematic analysis of multitude of variables including elements of DDS design and biological factors controlling its behavior *in vivo* is a daunting task (Fig.1).

In order to begin to examine some of the factors affecting this sort of drug delivery in a feasible way, we decided to focus on a one specific model system: delivery of the enzyme glucose oxidase (GOX) to the pulmonary circulation using antibodies to the endothelial surface antigen thrombomodulin (TM). We chose the pulmonary vasculature since the lungs contain ~30% of total endothelial surface in the body and, unlike other organs, receive the entire cardiac output of venous blood; hence DDSs targeted to endothelial cells accumulate in lungs [1,3,19,22, 39]. In addition, pulmonary endothelium is enriched in some determinant, including thrombomodulin [1,23,40–45]. Previous work showed that anti-TM/GOX targeting to the pulmonary endothelium results in rapid and easily measurable tissue damage due to the production of hydrogen peroxide from the ubiquitous substrates oxygen and glucose [18].

We first asked questions related to the characteristics of the antibodies and conjugates (Block 2, Figure 1). We have previously shown that the behavior and effects of antibody conjugates can be markedly different if they are directed against different endothelial antigens. For example, GOX targeting to platelet-endothelial adhesion molecule-1 (PECAM-1) *vs* TM causes distinct forms of pulmonary oxidative stress, since inhibition of these determinants causes different "side" effects: anti-TM/GOX injury is accompanied by thrombosis due to TM inhibition [18]. We have also shown that the size of the conjugates markedly affects the ability of the complex to target to the lungs [30].

In this study, we took advantage of two anti-TM monoclonal antibodies, mAbs anti-TM_{201} and anti-TM_{34} that non-competitively bind to distinct epitopes on murine TM [17,43]. We tested distribution of the radiolabeled TM antibodies and GOX conjugates one hour after IV injection. Previous studies of immunotargeting of radiolabeled conjugates directed to highly accessible endothelial determinants such as TM, angiotensin-converting enzyme (ACE), PECAM-1, intercellular adhesion molecule 1 (ICAM-1) and GP90 showed that their maximum uptake in the lungs occurs within 15-30 min, followed by a short 15–30 min stable period and subsequent reduction of the pulmonary level observed at times more than one hour after IV injection [22,25,27,46–52]. Therefore, the kinetics of lung edema development showing a maximum 4 hour after injection of a lower dose of the conjugate selected to avoid overt early lethality (Fig.4C) is not due to delayed accumulation of GOX in the lungs. Most likely, lag between peak anti-TM/GOX targeting and manifestation of its effect reveals the time interval that is necessary to generate sufficiently toxic amount of H_2O_2 in the pulmonary vasculature and cause the oxidative stress that takes a few hours to develop into vascular edema. Consistent with the fact that endothelium degrades delivered conjugates within a few hours [46,49,53], a more prolonged hyperoxia did not aggravate further the injury: enhanced supply of the substrate makes no difference when the targeted enzyme is gone.

Side-by-side comparison of anti-TM_{201} vs anti-TM_{34} and their conjugates showed that despite relatively comparable targeting of the unconjugated antibodies (Fig. 2A), one antibody (anti-TM_{201}) performed markedly better than the other antibody (anti-TM_{34}) when they served as affinity moieties of optimally-sized conjugates (Fig. 2B and 2C). The reasons for this marked difference are not entirely clear. Electron microscopy showed that anti-TM_{34} *vs* anti-TM_{201} preferentially binds to endothelial cells in thin *vs* thick alveolar walls, respectively [20]. *In vitro* studies showed that anti-TM_{201} has higher affinity to TM in endothelial cells, but lesser number of apparent binding sites in endothelial cells *vs* anti-TM_{34} (K_D approx 0.06 *vs* 0.56 nM and B_{max} approx 45 *vs* 150 fmoles, respectively). The higher affinity of anti-TM_{201}, as well as high susceptibility of mAb anti-TM_{34} to chemical modification [S. Kennel, unpublished data] may help to explain the higher efficiency of targeting of anti-TM_{201} *vs* anti-TM_{34} and their derivatives (Fig.2). The targeting effectiveness of anti-TM/GOX formulations (Fig.2B) correlated with their potency (Fig.3A). These studies indicate however, that the "rules" for choosing an optimally binding antibody to a specific epitope in a conjugate are not yet fully understood and still require empiric testing.

Once an optimal antibody is chosen, our data also show that variations in the drug delivery system (e.g., protein conjugates *vs* polymer carrier-based formulations) that include differences in structure, size, and activity of ingredients, may also affect delivery and effect of a cargo. For example, comparisons of protein anti-TM/GOX conjugates *vs* polymer nanospheres coated with the same anti-TM antibody and the same cargo (GOX) illustrate this point: anti-TM_{201}/bead/GOX showed the highest pulmonary targeting, double that of anti-TM_{201}/GOX streptavidin protein conjugates. This result may be explained by the fact that only a fraction of anti-TM is exposed on the surface of protein conjugates, while virtually all the anti-TM molecules are immobilized on the bead surface [24]. The multivalent nature of binding to

endothelial TM likely explains more effective targeting of conjugate and bead formulations of anti-TM_{201} (Fig. 2B,C) *vs* naked antibodies (Fig.2A).

We were also able to address questions related to the role of supply of an enzyme substrate in the target organ, taking advantage of the need for oxygen in the activity of glucose oxidase. Indeed, the substrate availability modulates local activity of targeted enzymes. This may be of importance in the future use of other oxygen-utilizing enzymes, e.g., prospective therapeutic enzyme nitric oxide synthase [54] or other non-enzymatic drugs, including some antibiotics and detoxifying agents utilizing oxygen as a co-factor. However, this principle will need to be kept in mind for any therapeutic enzyme.

Although effective binding to the target cells is necessary, it is not always sufficient to achieve the goal of targeting, i.e., attaining local effect of a cargo. A trivial example of this principal is shown in Figure 3, where the inadvertent inactivation of GOX absorbed on the surface of polymer nanocarriers led to a complete loss of tissue effects. Much more difficult to predict are other biologic variables that may alter the ultimate effect of the delivered drug. One such variable is the density of the antigen on the target organ. As shown in Figure 6, poorly understood variations in the expression levels of TM on the pulmonary vasculature of mice led to marked variations in the efficacy of the TM/GOX conjugate. These studies point out the importance of testing drug delivery in disease models similar to those being targeted and not only in unperturbed “normal” animals.

Factors underlying individual variability will likely be of even greater importance in the therapeutic and adverse effects of pharmacotherapy in humans. Because patients respond variably to drugs, in terms of both therapeutic and adverse effects, it is important to develop strategies that could optimize the selection and dosing of pharmacological agents for a given individual. These challenges actually exist for almost all drugs, however drug targeting has the great advantage that many of these issues can be specifically localized, addressed and optimized. This study has begun this process by showing how targeting and effects of pharmacological cargoes are controlled by systemic and local biological factors such as the specific antibody used, substrate availability, variations in target antigen availability, and biologic differences in response to the same drug. A better of understanding of these variables will inevitably lead to improvements in future drug delivery systems design.

Acknowledgements

We thank Drs. Michael Koval, Silvia Muro and Thomas Dziubla for helpful discussions and Dr. Benjamin Jackson and John Lawson for isoprostane measurements. This work was supported in part by National Institutes of Health Grants NHLBI RO1 HL71175, HL078785 and HL73940 and Department of Defense Grant PR 012262 (VRM).

References

1. Muzykantov VR. Biomedical aspects of targeted delivery of drugs to pulmonary endothelium. Expert Opin Drug Deliv 2005;2:909–926. [PubMed: 16296786]
2. Everts M, Kok RJ, Asgeirsdottir SA, Melgert BN, Moolenaar TJ, Koning GA, van Luyn MJ, Meijer DK, Molema G. Selective intracellular delivery of dexamethasone into activated endothelial cells using an E-selectin-directed immunoconjugate. J Immunol 2002;168:883–889. [PubMed: 11777986]
3. Li S, Tan Y, Viroonchatapan E, Pitt BR, Huang L. Targeted gene delivery to pulmonary endothelium by anti-PECAM antibody. Am J Physiol Lung Cell Mol Physiol 2000;278:L504–511. [PubMed: 10710522]
4. Davda J, Labhasetwar V. Characterization of nanoparticle uptake by endothelial cells. Int J Pharm 2002;233:51–59. [PubMed: 11897410]
5. Mennesson E, Erbacher P, Kuzak M, Kieda C, Midoux P, Pichon C. DNA/cationic polymer complex attachment on a human vascular endothelial cell monolayer exposed to a steady laminar flow. J Control Release 2006;114:389–397. [PubMed: 16887230]

6. Rychak JJ, Lindner JR, Ley K, Klibanov AL. Deformable gas-filled microbubbles targeted to P-selectin. J Control Release 2006;114:288–299. [PubMed: 16887229]
7. Tirand L, Frochot C, Vanderesse R, Thomas N, Trinquet E, Pinel S, Viriot ML, Guillemin F, Barberi-Heyob M. A peptide competing with VEGF165 binding on neuropilin-1 mediates targeting of a chlorin-type photosensitizer and potentiates its photodynamic activity in human endothelial cells. J Control Release 2006;111:153–164. [PubMed: 16423422]
8. Ding BS, Dziubla T, Shuvaev VV, Muro S, Muzykantov VR. Advanced drug delivery systems that target the vascular endothelium. Mol Interv 2006;6:98–112. [PubMed: 16565472]
9. Bronich TK, Ouyang M, Kabanov VA, Eisenberg A, Szoka FC Jr, Kabanov AV. Synthesis of vesicles on polymer template. J Am Chem Soc 2002;124:11872–11873. [PubMed: 12358530]
10. Gref R, Minamitake Y, Peracchia MT, Trubetskoy V, Torchilin V, Langer R. Biodegradable long-circulating polymeric nanospheres. Science 1994;263:1600–1603. [PubMed: 8128245]
11. Kiani MF, Yuan H, Chen X, Smith L, Gaber MW, Goetz DJ. Targeting microparticles to select tissue via radiation-induced upregulation of endothelial cell adhesion molecules. Pharm Res 2002;19:1317–1322. [PubMed: 12403068]
12. Ahmed F, Pakunlu RI, Brannan A, Bates F, Minko T, Discher DE. Biodegradable polymersomes loaded with both paclitaxel and doxorubicin permeate and shrink tumors, inducing apoptosis in proportion to accumulated drug. J Control Release. 2006
13. Crommelin DJ, Storm G, Jiskoot W, Stenekes R, Mastrobattista E, Hennink WE. Nanotechnological approaches for the delivery of macromolecules. J Control Release 2003;87:81–88. [PubMed: 12618025]
14. Pakunlu RI, Wang Y, Saad M, Khandare JJ, Starovoytov V, Minko T. In vitro and in vivo intracellular liposomal delivery of antisense oligonucleotides and anticancer drug. J Control Release. 2006
15. Orfanos SE, Langleben D, Khoury J, Schlesinger RD, Dragatakis L, Roussos C, Ryan JW, Catravas JD. Pulmonary capillary endothelium-bound angiotensin-converting enzyme activity in humans. Circulation 1999;99:1593–1599. [PubMed: 10096936]
16. Vogel SM, Minshall RD, Pilipovic M, Tiruppathi C, Malik AB. Albumin uptake and transcytosis in endothelial cells in vivo induced by albumin-binding protein. Am J Physiol Lung Cell Mol Physiol 2001;281:L1512–1522. [PubMed: 11704548]
17. Kennel SJ, Lankford T, Hughes B, Hotchkiss JA. Quantitation of a murine lung endothelial cell protein, P112, with a double monoclonal antibody assay. Lab Invest 1988;59:692–701. [PubMed: 2460698]
18. Christofidou-Solomidou M, Kennel S, Scherpereel A, Wiewrodt R, Solomides CC, Pietra GG, Murciano JC, Shah SA, Ischiropoulos H, Albelda SM, Muzykantov VR. Vascular immunotargeting of glucose oxidase to the endothelial antigens induces distinct forms of oxidant acute lung injury: targeting to thrombomodulin, but not to PECAM-1, causes pulmonary thrombosis and neutrophil transmigration. Am J Pathol 2002;160:1155–1169. [PubMed: 11891211]
19. Christofidou-Solomidou M, Scherpereel A, Wiewrodt R, Ng K, Sweitzer T, Arguiri E, Shuvaev V, Solomides CC, Albelda SM, Muzykantov VR. PECAM-directed delivery of catalase to endothelium protects against pulmonary vascular oxidative stress. Am J Physiol Lung Cell Mol Physiol 2003;285:L283–292. [PubMed: 12851209]
20. Rorvik MC, Allison DP, Hotchkiss JA, Witschi HP, Kennel SJ. Antibodies to mouse lung capillary endothelium. J Histochem Cytochem 1988;36:741–749. [PubMed: 3290332]
21. Kennel SJ, Falcioni R, Wesley JW. Microdistribution of specific rat monoclonal antibodies to mouse tissues and human tumor xenografts. Cancer Res 1991;51:1529–1536. [PubMed: 1997194]
22. Muzykantov VR, Christofidou-Solomidou M, Balyasnikova I, Harshaw DW, Schultz L, Fisher AB, Albelda SM. Streptavidin facilitates internalization and pulmonary targeting of an anti-endothelial cell antibody (platelet-endothelial cell adhesion molecule 1): a strategy for vascular immunotargeting of drugs. Proc Natl Acad Sci U S A 1999;96:2379–2384. [PubMed: 10051650]
23. Muzykantov VR, Atochina EN, Ischiropoulos H, Danilov SM, Fisher AB. Immunotargeting of antioxidant enzyme to the pulmonary endothelium. Proc Natl Acad Sci U S A 1996;93:5213–5218. [PubMed: 8643555]

24. Shuvaev VV, Dziubla T, Wiewrodt R, Muzykantov VR. Streptavidin-biotin crosslinking of therapeutic enzymes with carrier antibodies: nanoconjugates for protection against endothelial oxidative stress. Methods Mol Biol 2004;283:3–19. [PubMed: 15197299]
25. Christofidou-Solomidou M, Pietra GG, Solomides CC, Arguiris E, Harshaw D, Fitzgerald GA, Albelda SM, Muzykantov VR. Immunotargeting of glucose oxidase to endothelium in vivo causes oxidative vascular injury in the lungs. Am J Physiol Lung Cell Mol Physiol 2000;278:L794–805. [PubMed: 10749757]
26. Muro S, Wiewrodt R, Thomas A, Koniaris L, Albelda SM, Muzykantov VR, Koval M. A novel endocytic pathway induced by clustering endothelial ICAM-1 or PECAM-1. J Cell Sci 2003;116:1599–1609. [PubMed: 12640043]
27. Muro S, Dziubla T, Qiu W, Leferovich J, Cui X, Berk E, Muzykantov VR. Endothelial targeting of high-affinity multivalent polymer nanocarriers directed to intercellular adhesion molecule 1. J Pharmacol Exp Ther 2006;317:1161–1169. [PubMed: 16505161]
28. Freitas S, Merkle HP, Gander B. Microencapsulation by solvent extraction/evaporation: reviewing the state of the art of microsphere preparation process technology. J Control Release 2005;102:313–332. [PubMed: 15653154]
29. Niwa T, Takeuchi H, Hino T, Kunou N, Kawashima Y. Preparations of biodegradable nanospheres of water-soluble and insoluble drugs with -lactide/glycolide copolymer by a novel spontaneous emulsification solvent diffusion method, and the drug release behavior. J Control Release 1993;25:89–98.
30. Wiewrodt R, Thomas AP, Cipelletti L, Christofidou-Solomidou M, Weitz DA, Feinstein SI, Schaffer D, Albelda SM, Koval M, Muzykantov VR. Size-dependent intracellular immunotargeting of therapeutic cargoes into endothelial cells. Blood 2002;99:912–922. [PubMed: 11806994]
31. Laemmli UK. Cleavage of structural proteins during the assembly of the head of bacteriophage T4. Nature 1970;227:680–685. [PubMed: 5432063]
32. Christofidou-Solomidou M, Scherpereel A, Solomides CC, Muzykantov VR, Machtay M, Albelda SM, DiNubile MJ. Changes in plasma gelsolin concentration during acute oxidant lung injury in mice. Lung 2002;180:91–104. [PubMed: 12172902]
33. Perkowski S, Scherpereel A, Murciano JC, Arguiri E, Solomides CC, Albelda SM, Muzykantov V, Christofidou-Solomidou M. Dissociation between Alveolar Transmigration of Neutrophils and Lung Injury in Hyperoxia. Am J Physiol Lung Cell Mol Physiol. 2006
34. Kou JH, Emmett C, Shen P, Aswani S, Iwamoto T, Vaghefi F, Cain G, Sanders L. Bioerosion and biocompatibility of poly(d,l-lactic-co-glycolic acid) implants in brain. J Controll Release 1997;43:123–130.
35. Yamaguchi K, Anderson JM. In vivo biocompatibility studies of medisorb(R) 65/35 D,L-lactide/glycolide copolymer microspheres. J Control Release 1993;24:81–93.
36. Zweers ML, Engbers GH, Grijpma DW, Feijen J. Release of anti-restenosis drugs from poly(ethylene oxide)-poly(DL-lactic-co-glycolic acid) nanoparticles. J Control Release 2006;114:317–324. [PubMed: 16884807]
37. Crapo JD. Morphologic changes in pulmonary oxygen toxicity. Annu Rev Physiol 1986;48:721–731. [PubMed: 3518622]
38. Moore KL, Esmon CT, Esmon NL. Tumor necrosis factor leads to the internalization and degradation of thrombomodulin from the surface of bovine aortic endothelial cells in culture. Blood 1989;73:159–165. [PubMed: 2535943]
39. Muro S, Muzykantov VR. Targeting of antioxidant and anti-thrombotic drugs to endothelial cell adhesion molecules. Curr Pharm Des 2005;11:2383–2401. [PubMed: 16022673]
40. Danilov SM, Gavrilyuk VD, Franke FE, Pauls K, Harshaw DW, McDonald TD, Miletich DJ, Muzykantov VR. Lung uptake of antibodies to endothelial antigens: key determinants of vascular immunotargeting. Am J Physiol Lung Cell Mol Physiol 2001;280:L1335–1347. [PubMed: 11350815]
41. Oh P, Li Y, Yu J, Durr E, Krasinska KM, Carver LA, Testa JE, Schnitzer JE. Subtractive proteomic mapping of the endothelial surface in lung and solid tumours for tissue-specific therapy. Nature 2004;429:629–635. [PubMed: 15190345]

42. Pasqualini R, Arap W, McDonald DM. Probing the structural and molecular diversity of tumor vasculature. Trends Mol Med 2002;8:563–571. [PubMed: 12470989]
43. Ford VA, Stringer C, Kennel SJ. Thrombomodulin is preferentially expressed in Balb/c lung microvessels. J Biol Chem 1992;267:5446–5450. [PubMed: 1372003]
44. McIntosh DP, Tan XY, Oh P, Schnitzer JE. Targeting endothelium and its dynamic caveolae for tissue-specific transcytosis in vivo: a pathway to overcome cell barriers to drug and gene delivery. Proc Natl Acad Sci U S A 2002;99:1996–2001. [PubMed: 11854497]
45. Schnitzer JE. Caveolae: from basic trafficking mechanisms to targeting transcytosis for tissue-specific drug and gene delivery in vivo. Adv Drug Deliv Rev 2001;49:265–280. [PubMed: 11551399]
46. Kozower BD, Christofidou-Solomidou M, Sweitzer TD, Muro S, Buerk DG, Solomides CC, Albelda SM, Patterson GA, Muzykantov VR. Immunotargeting of catalase to the pulmonary endothelium alleviates oxidative stress and reduces acute lung transplantation injury. Nat Biotechnol 2003;21:392–398. [PubMed: 12652312]
47. Muzykantov VR, Atochina EN, Kuo A, Barnathan ES, Notarfrancesco K, Shuman H, Dodia C, Fisher AB. Endothelial cells internalize monoclonal antibody to angiotensin-converting enzyme. Am J Physiol 1996;270:L704–713. [PubMed: 8967503]
48. Muzykantov VR, Barnathan ES, Atochina EN, Kuo A, Danilov SM, Fisher AB. Targeting of antibody-conjugated plasminogen activators to the pulmonary vasculature. J Pharmacol Exp Ther 1996;279:1026–1034. [PubMed: 8930213]
49. Scherpereel A, Wiewrodt R, Christofidou-Solomidou M, Gervais R, Murciano JC, Albelda SM, Muzykantov VR. Cell-selective intracellular delivery of a foreign enzyme to endothelium in vivo using vascular immunotargeting. Faseb J 2001;15:416–426. [PubMed: 11156957]
50. Murciano JC, Harshaw DW, Ghitescu L, Danilov SM, Muzykantov VR. Vascular immunotargeting to endothelial surface in a specific macrodomain in alveolar capillaries. Am J Respir Crit Care Med 2001;164:1295–1302. [PubMed: 11673225]
51. Muro S, Gajewski C, Koval M, Muzykantov VR. ICAM-1 recycling in endothelial cells: a novel pathway for sustained intracellular delivery and prolonged effects of drugs. Blood 2005;105:650–658. [PubMed: 15367437]
52. Ding BS, Gottstein C, Grunow A, Kuo A, Ganguly K, Albelda SM, Cines DB, Muzykantov VR. Endothelial targeting of a recombinant construct fusing a PECAM-1 single-chain variable antibody fragment (scFv) with prourokinase facilitates prophylactic thrombolysis in the pulmonary vasculature. Blood 2005;106:4191–4198. [PubMed: 16144802]
53. Muro S, Cui X, Gajewski C, Murciano JC, Muzykantov VR, Koval M. Slow intracellular trafficking of catalase nanoparticles targeted to ICAM-1 protects endothelial cells from oxidative stress. Am J Physiol Cell Physiol 2003;285:C1339–1347. [PubMed: 12878488]
54. Miller WH, Brosnan MJ, Graham D, Nicol CG, Morecroft I, Channon KM, Danilov SM, Reynolds PN, Baker AH, Dominiczak AF. Targeting endothelial cells with adenovirus expressing nitric oxide synthase prevents elevation of blood pressure in stroke-prone spontaneously hypertensive rats. Mol Ther 2005;12:321–327. [PubMed: 16043100]

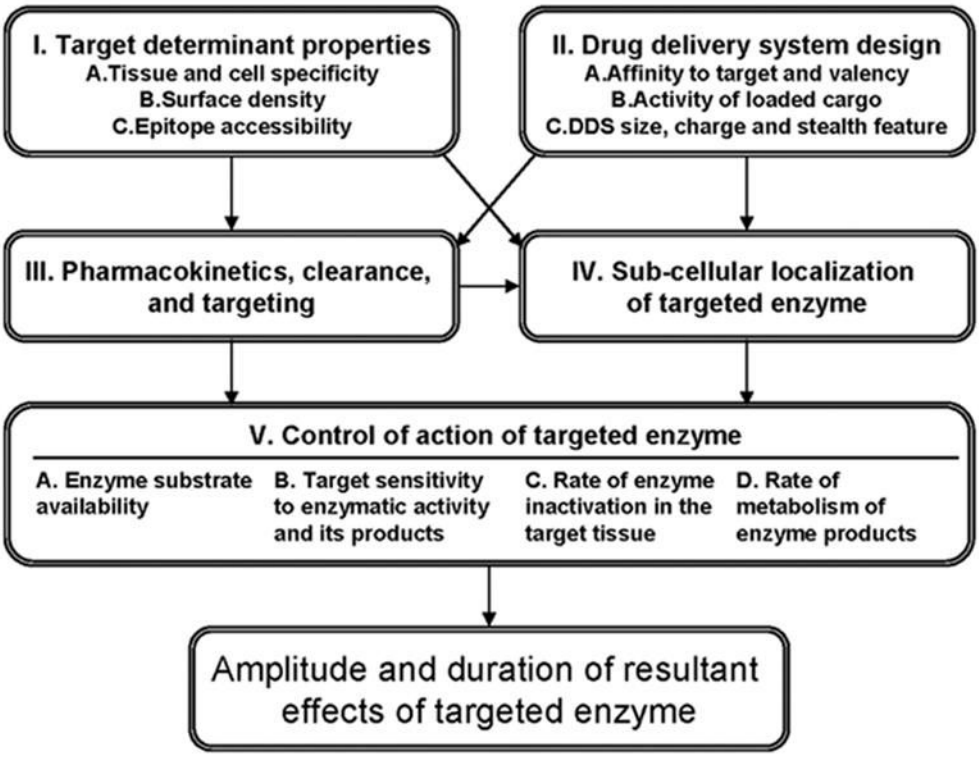

Fig. 1.

Drug delivery systems (DDS) for endothelial targeting of therapeutic enzymes. This schematic flowchart illustrates parameters that control targeting and effects of an enzyme cargo. Thus, DDS circulation is controlled by its size and charge. Targeting is controlled by features of a target determinant and DDS affinity. Sub-cellular localization of a drug is controlled by features of the selected target determinant, valence and size of DDS. These factors and biological features of the target tissue (Block V) modulate the outcome effects of targeted enzymes.

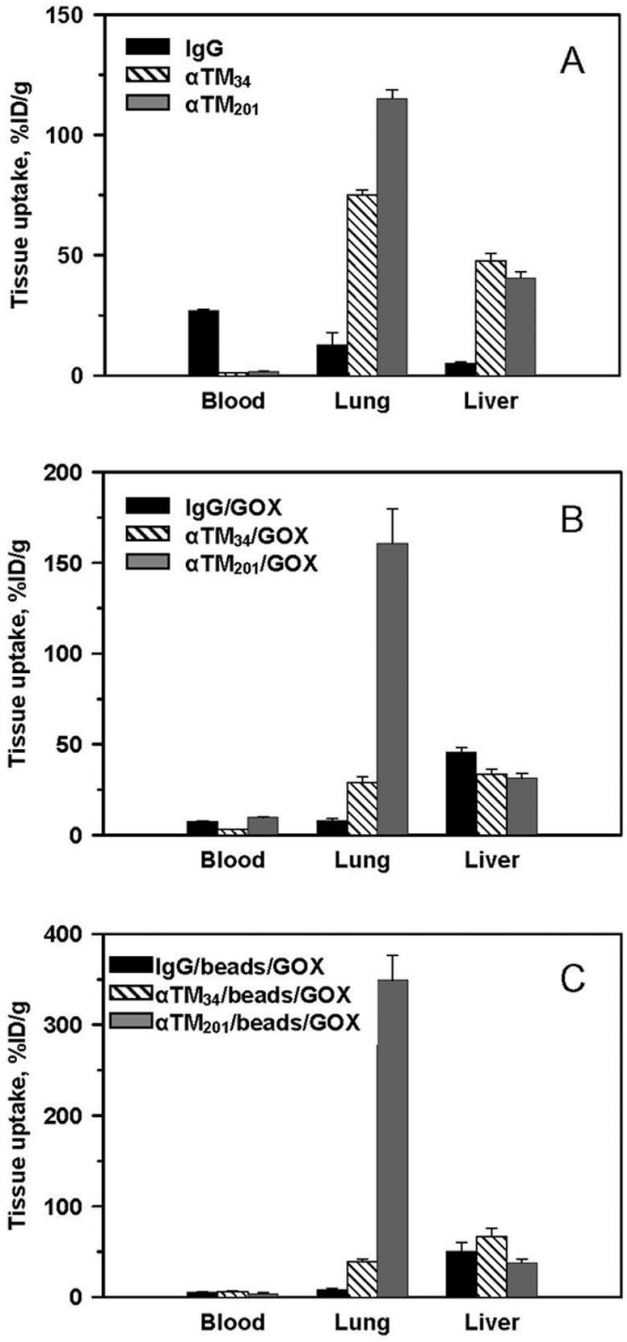

Fig. 2.

Targeting of anti-TM/GOX formulations to pulmonary vasculature after intravenous injection in mice. Tissue levels of ^{125}Iodine 1 hour after IV injection of radiolabeled monoclonal antibodies and their formulations. Hatch bars: anti-TM_{34}, gray bars: anti-TM_{201}, black bars: irrelevant control IgG. Tissue distribution is shown as percent of injected dose per gram of tissue (%ID/g) of: ^{125}I-labeled anti-TM (A); anti-TM conjugated with ^{125}I-GOX via streptavidin-biotin cross-linking (B); and anti-TM-coated beads co-coated with ^{125}I-GOX (C). Unless specified otherwise, in this and subsequent figures the data are shown as mean ± SEM, $n \geq 3$.

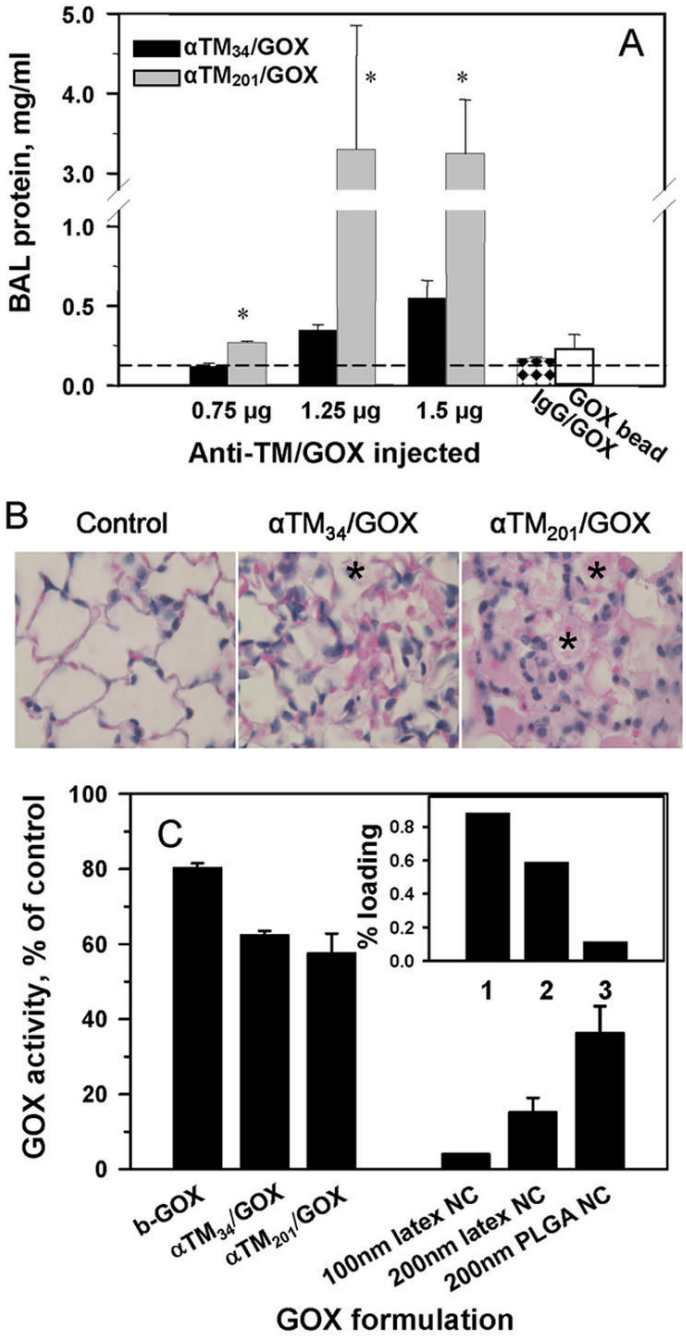

Fig. 3.

Delivery efficacy and enzymatic activity of anti-TM/GOX formulations control their effect in the target tissue manifested in vivo by edematous lung injury. Panel A: protein level in the BAL fluid reflecting alveolar edema caused by oxidative stress by H_2O_2 produced by GOX were determined 4 hours after injection of indicated doses of anti-TM_{34}/GOX (black bars) or anti-TM_{201}/GOX (gray bars). Right bars show effects of 2.0 μg/kg control IgG/GOX (checkered bar) or anti-TM_{201}/bead/GOX (open bar). Asterisk: difference *vs* adjacent bar and background level of BAL protein in naïve mice (indicated by dash line) is significant at $p<0.05$. Panel B: pathological alterations in the lung tissue sections 4 hours after injection of 1.5 μg/kg of indicated preparations. Note accumulation of leukocytes and protein-rich edematous

liquid in the alveoli depicted by asterisks. Panel C. Effect of biotinylation, conjugation and coating to polystyrene and PLGA nanoparticles on GOX activity. Inset: loading of radiolabeled GOX in polystyrene and PLGA nanoparticles: (1), 100 nm latex NC; (2), 200 nm latex NC; (3), 200 nm PLGA NC.

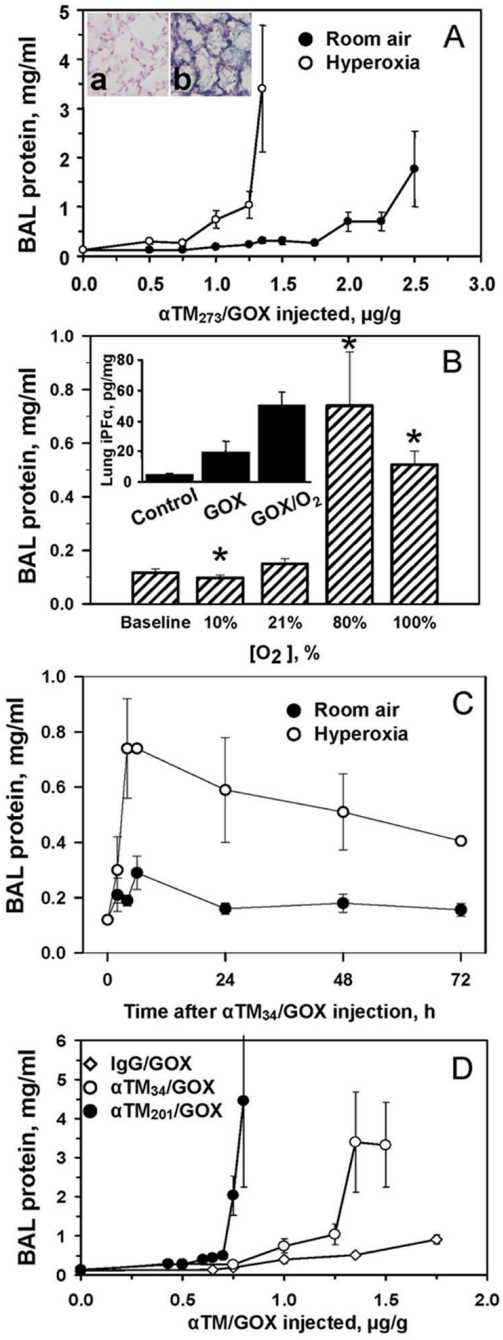

Fig. 4.

Level of oxygen modulates effect of anti-TM/GOX in accumulated in mouse pulmonary vasculature. Panel A. Alveolar edema detected 4 hours after injection of anti-TM_{34}/GOX at room air (closed circles) *vs* 80% O_2 (open circles). Inset shows immunostaining for a marker of oxidative injury, nitrotyrosine, in lungs exposed to room air (left) *vs* hyperoxia (right). Panel B. Extent of lung injury 4 hours after injection of 1.25 μg/g of anti-TM_{34}/GOX is proportional to rate of oxygen supply. Asterisk: difference of hypoxia or hyperoxia *vs* room air is significant at $p<0.05$. Inset: hyperoxia augments level of a marker of lipid peroxidation, iPF2α isoprostane in the lung homogenates. Panel C. Kinetics of lung injury after the injection of 1.25 μg/g of anti-TM_{34}/GOX at room (closed circles) air *vs* 80% O_2 (open circles). Panel D. Alveolar edema

4 hours after injection of indicated doses of control non-targeted IgG/GOX (diamonds) *vs* anti-TM_{34}/GOX (open circles) or anti-TM_{201}/GOX (closed circles) conjugates at 80% O_2.

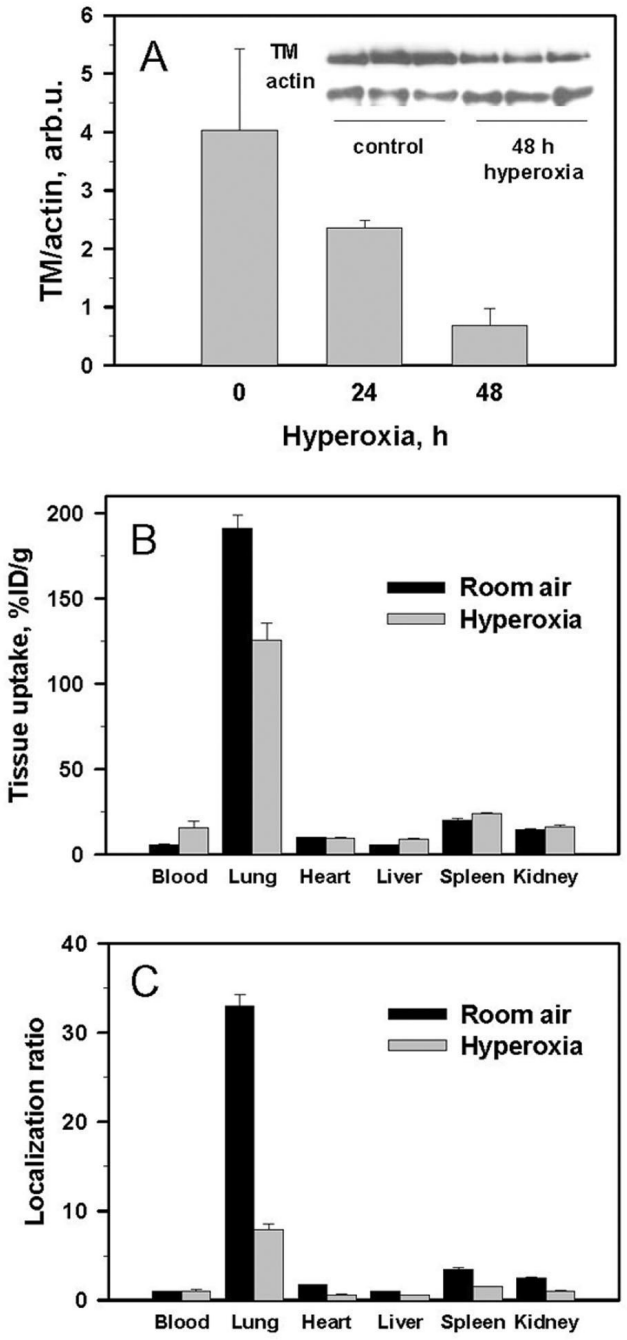

Fig. 5.

Pathophysiological factors (oxidative stress induced by prolonged hyperoxia) modulate pulmonary TM expression and targeting of anti-TM. Panel A: Western-blotting of TM expression in the lung tissue homogenates in mice exposed to hyperoxia for 0, 24 or 48 hours. Panel B: Pulmonary uptake of ^{125}I-anti-TM 1 hour after injection in mice exposed for 48 hours to room air (black bars) or hyperoxia (light bars). Panel C: data shown in the panel B represented as organ-to-blood ratio, which accounts for differences in blood level of circulating radiolabeled antibody.

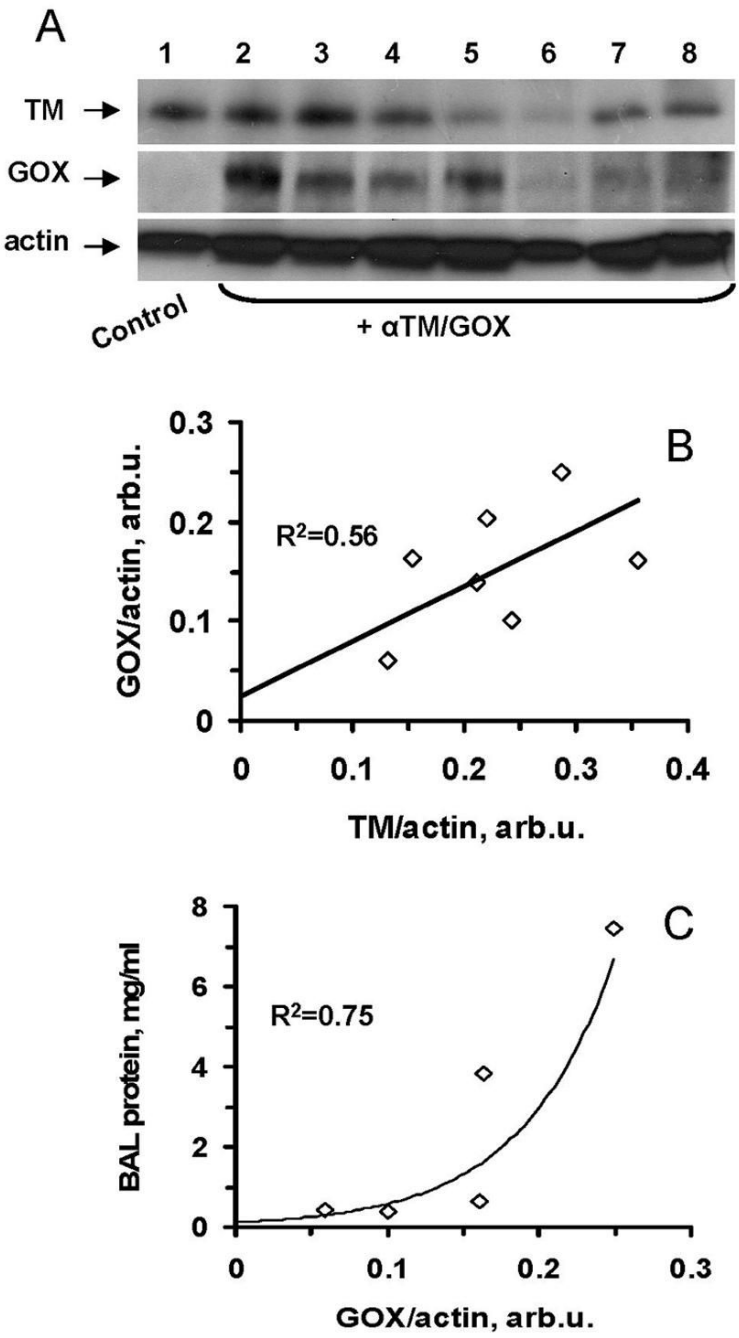

Fig. 6.

Anti-TM/GOX pulmonary targeting and effect correlate with level of TM expression. Panel A: Western blotting analysis of lung TM and GOX four hours after anti-TM/GOX injection. Panels B and C: correlations of lung TM level *vs* GOX delivery (B) and GOX delivery *vs* lung injury (C).